Computing Extreme Origami Bases

Erik D. Demaine and Martin L. Demaine
Dept. of Computer Science
University of Waterloo
Waterloo, Ontario, Canada N2L 3G1
{eddemaine,mldemaine}@daisy.uwaterloo.ca

December 18, 1997

Abstract

In this paper, we examine *extreme origami bases* that fold the boundary of a polygonal sheet of paper to a common plane, generalizing the Husimi and Meguro molecules used in origami design. This also solves the *folding-and-cutting problem*, where we want to make a specified polygon by one complete straight cut after arbitrary folding of a square sheet of paper. We present an algorithm to construct the crease pattern of an extreme base for paper in the shape of an arbitrary simple polygon. It is based on the straight skeleton, a variant on the medial axis. For convex polygons, we describe exactly how the folding process can be performed. This proves that the folding can even be done with paper that is rigid except at the creases, and allows animation of the folding process. Such descriptions have not been achieved before for an infinite class of origamis.

1 Introduction

Origami mathematics is the study of the geometry and other properties of origami (paper folding). The area of origami mathematics is still in its infancy, having only been seriously studied for the past seventeen years [10]. Geretschläger [7] and Huzita and Scimemi [11] examined the geometric constructions possible with origami, and compared them to a ruler and compass. Bern and Hayes [3] showed that it is $\mathcal{NP}$-hard to determine if a crease pattern (Section 2) is flat foldable, as is computing a flat folding (overlap order) given a suitable direction of folds (mountain and valley assignment). Hull [9] and Kawasaki [13] focus on necessary and sufficient conditions for flat foldability of crease patterns with a single vertex, which are also necessary conditions for general crease patterns. Justin [12] examines

necessary and sufficient conditions on overlap orders, resulting in a characterization of flat foldability for general crease patterns.

Lang has taken the most algorithmic approach. In [14], he describes an algorithm to construct "uniaxial" bases (see Section 2), which can then be folded into arbitrarily complex models. This solves a major problem in origami sekkei, or technical folding.

1.1 Extreme Bases

We are interested in a special kind of uniaxial base, which we call an *extreme base*, that folds the boundary of the paper onto a common plane, while the rest of the paper lies above and is perpendicular to this plane. This problem has been solved when the paper is a triangle and a convex quadrilateral by Husimi and Meguro, respectively [17]; these two "molecules" are the basis for much origami design. Our goal in this paper is to generalize these results to any polygonal sheet of paper, that is, constructively prove the following.

Theorem 1 *Any sheet of paper in the shape of a polygon $\mathcal{P}$ can be folded into an extreme base.*

More specifically, in this paper we present an algorithm to find the crease pattern of such a base, given an arbitrary polygon $\mathcal{P}$. For convex polygons, we describe the entire folding process using paper that is rigid in each face outlined by creases. Such a construction for an infinite class of origamis (parameterized by the polygon $\mathcal{P}$) has not been achieved before. For non-convex polygons, we know that rigidity is not possible, that is the paper must curve, so a description of the folding process is perhaps less informative. Instead, we are currently working on a description of the folded state, which would rigorously prove Theorem 1 in this case.

Figure 1 shows snapshots from three of the animations resulting from our algorithm.

1.2 Folding-and-Cutting Problem

The original application for this problem is what we call the folding-and-cutting problem, where one complete straight cut is allowed after arbitrary folding, typically starting from a square piece of paper. Using this single cut, the unfolded pieces can have a variety of shapes. This has been used for a magic trick by Houdini [8] before he became a famous escape artist, and was recreationally studied in detail by magician Loe [15]. Gardner [6] wrote briefly about this problem, posing it as an open question to cut out complex polygons.

In general, the problem is to arrange the folding so as to cut along an arbitrary arrangement of line segments, and no more. In this paper, we consider a special case of the problem, where the line segments form a polygon $\mathcal{P}$. This means that we want to fold the square paper flat so that the boundary of $\mathcal{P}$ maps to a common line, and nothing else maps to this line; we can then simply cut along this line.
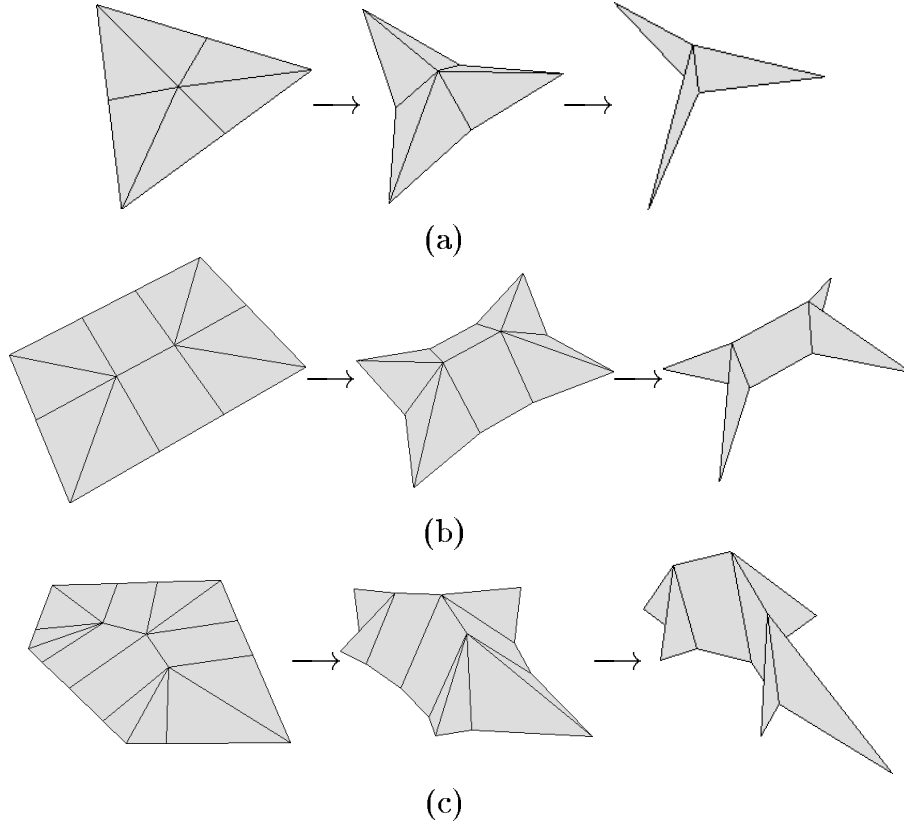
Figure 1: *Unfolded, partially folded, and completely folded extreme bases for (a) a triangle, (b) a convex quadrilateral, and (c) a convex pentagon. Note that these pictures are drawn with a perspective transformation.*

By Theorem 1, we can construct an extreme base for a sheet of paper with shape $\mathcal{P}$. As we will see in Lemma 9, this can then be "flattened" to lie on a plane, where the boundary of $\mathcal{P}$ is on a line. If $\mathcal{P}$ is convex, we can extend the creases at the vertices of $\mathcal{P}$ (which are angular bisectors) until they reach the end of the square paper. No crossing will occur since the angular bisectors all go "outward" from a convex polygon. Hence, we obtain a flat folding that maps the boundary of $\mathcal{P}$ to a common line.

Theorem 2 *Given any convex polygon $\mathcal{P}$ drawn on a sheet of paper, the paper can be folded into a flat origami such that the boundary of $\mathcal{P}$ maps to a common line, and nothing else maps to that line.*

1.3 Outline

The rest of this paper is outlined as follows. Section 2 provides a background in origami mathematics by defining crease patterns, bases, and extreme bases. In Section 3, we briefly

describe the straight skeleton, a variant on the medial axis. In Section 4, we use the straight skeleton to define our crease pattern. Section 5 shows how the folding process can be completely described for convex polygons. Finally, we conclude in Section 6.

2   Background

A *crease pattern* is a division of the paper $\mathcal{P}$, a (simple) polygon in the plane, into a finite number of sub-polygons, called *faces*. Each edge corresponds to a crease. Given a crease pattern, a *base* [3, 9, 14] is a folded version of the paper. That is, a base is a continuous piecewise-isometric function b from $\mathcal{P}$ to 3-space. Here "piecewise isometric" means that b is an isometry when restricted to any face of the crease pattern.

We are also interested in the process f of folding the flat paper into a base b. To do this, we introduce the notion of a time t in the interval $[0, 1]$. A folding is then a continuous function f from $\mathcal{P} \times [0, 1]$ to 3-space. The initial time $t = 0$ represents the initial flat sheet of paper (that is, the unfolded state), and the final time $t = 1$ represents the final folded base (that is, the folded state). Formally, for any $p \in \mathcal{P}$, $f(p, 0) = (p, 0)^1$ and $f(p, 1) = b(p)$.

In between the endpoints in time, we must enforce some properties to ensure that the folding is valid. First, f cannot stretch the paper. For our purposes, we do not allow curving, so this is equivalent to forcing that f must be piecewise isometric for every fixed time; that is, f restricted to any face and time $0 \leq t \leq 1$ must be an isometry. Second, f cannot force the paper to cross through itself, an event called ripping. We will use a stronger property that once two "molecules" of paper touch, they are permanently joined. Formally, if $f(p, t) = f(q, t)$ then $f(p, s) = f(q, s)$ for all $t < s \leq 1$. Note that this is satisfied if f is one-to-one for every fixed $t < 1$.

Conceptually, one could discretize f slightly and use this as "instructions" on how to fold the base. In particular, we can animate the folding process.

Our target area of origami is *flat origami*. We are implicitly dealing with such origamis, for example in the folding-and-cutting problem. A base b is *flat* if the image $b(\mathcal{P})$ lies on a plane. A *flat folding* is a folding into a flat base.

Lang [14] defines a *uniaxial base* b as follows. First, $b^z(p)$ must be non-negative for all points $p \in \mathcal{P}$. Second, the projection of the base onto the xy ($z = 0$) plane must equal the intersection of the base with the xy plane, that is, we must have

$$\{b(p) \mid p \in \mathcal{P}, b^z(p) = 0\} = \{(b^{xy}(p), 0) \mid p \in \mathcal{P}\}.$$

Furthermore, this set must form a tree, so we call it the *shadow tree*. Hence, b maps each face of the crease pattern so that it is perpendicular to the xy plane. Finally, each face must belong to a unique *flap*, a maximal set F of faces that project to a common edge of the shadow tree, with the added property that the boundary of each $f \in F$ projects to one or both of the endpoints of this edge.

---

[1]$(p, 0)$ is shorthand for the point $(p^x, p^y, 0)$ in 3-space, where p is the point (p^x, p^y) in 2-space.
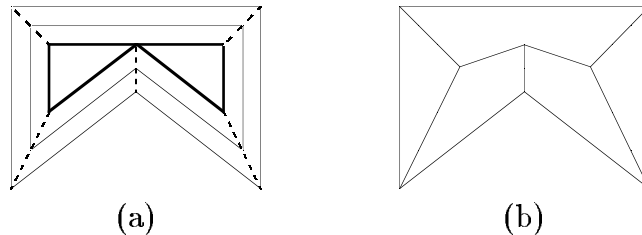
Figure 2: *(a) Two shrunken polygons of the original. The second, drawn in bold, is degenerate. Trajectories of the vertices are dashed. (b) Complete straight skeleton.*

We believe a more useful definition of uniaxial, which we use in this paper, is a generalization to arbitrary planes parallel to the xy plane. We enforce that, for any $c \geq 0$,

$$\{b(p) \mid p \in \mathcal{P}, b^z(p) = c\} = \{(b^{xy}(p), c) \mid p \in \mathcal{P}, b^z(p) \geq c\}.$$

This means that if we cut the base parallel to the xy plane (removing the portion below the cut plane), then the result is also uniaxial by Lang's definition [14] described above.

We call a base b *extreme* if it is uniaxial and $b(p) = 0$ if and only if p is on the boundary of $\mathcal{P}$. The goal of this paper is to present an algorithm to compute an extreme base for paper in the shape of an arbitrary polygon $\mathcal{P}$, and hence constructively prove Theorem 1.

3   Straight Skeleton

In this section, we briefly look at a structure called the *straight skeleton*, which consists of the main folds for our extreme bases.

For convex polygons $\mathcal{P}$, the straight skeleton is equivalent to the *medial axis* [4, 18]. Conceptually, if we light a prairie fire along the boundary of the polygon, then the medial axis is where the fire meets and burns itself out. With the straight skeleton, fire does not spread in a circular (Euclidean) way. Instead, we uniformly shrink the polygon until it becomes non-simple; we then recursively shrink each sub-polygon, unless it has zero area. The straight skeleton consists of the trajectories of the vertices of the polygon and sub-polygons during this process.

An example of the shrinking process is given in Figure 2(a). The polygon becomes non-simple when it shrinks down to two triangles. Continuing the shrinking in each triangle generates the angular bisectors until they meet (Figure 2(b)).

Figure 3 shows both the straight skeleton and the medial axis for a hexagon. This proves that the straight skeleton is not just a local "straightening out" of the medial axis; they can be topologically different. Aichholzer et al. [2] prove that the straight skeleton can in fact be described using asymptotically fewer bits than the medial axis.

Lord and Wilson [16, pp. 98–101] are the first we know of to examine the straight skeleton, and consider it for curved shapes. Aichholzer et al. [2], who coined the term straight skeleton,
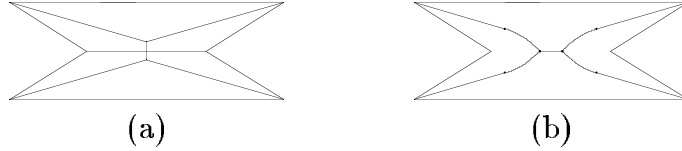
Figure 3: *(a) Straight skeleton and (b) medial axis of the same polygon, illustrating that they may be topologically different.*

are the first to publish an algorithm to calculate the straight skeleton of a polygon, running in $O(n^2 \log n)$ time. Aichholzer and Aurenhammer [1] generalized this result to general polygonal subdivisions of the plane. Eppstein and Erickson recently achieved an $O(n^{17/11+\epsilon})$ algorithm [5].

We will denote the straight skeleton of $\mathcal{P}$ by $\mathrm{SS}(\mathcal{P})$ or simply SS. Let $V(\mathrm{SS})$, $L(\mathrm{SS})$, $I(\mathrm{SS})$, $E(\mathrm{SS})$ denote the set of vertices, leaf (degree-1) vertices, internal (non-leaf) vertices, and edges of SS, respectively. We now state some properties of the straight skeleton that we will use later in the paper.

Lemma 1 [2] *Each edge $e \in E(\mathrm{SS}(\mathcal{P}))$ is a line segment; unlike the medial axis, the straight skeleton does not curve). Furthermore, SS forms a tree, that is, $|E(\mathrm{SS})| = |V(\mathrm{SS})| - 1$. Every $v \in L(\mathrm{SS})$ is a vertex of $\mathcal{P}$, and every vertex of $\mathcal{P}$ is $\in L(\mathrm{SS})$. SS divides $\mathcal{P}$ into $|E(\mathrm{SS})|$ regions, each incident to a different edge of $\mathcal{P}$.*

We choose to root the straight-skeleton tree at the vertex $r = \mathrm{root}(\mathrm{SS}) \in I(\mathrm{SS})$ formed from the last shrinking of a sub-polygon of $\mathcal{P}$ down to a point. (Note that we often assume that $\mathrm{root}(\mathrm{SS})$ is unique; otherwise, $\mathcal{P}$ is degenerate in that two shrinking events occurred simultaneously.) Rooting at r defines a parent map in the obvious way.

A *bisector graph* [2] of $\mathcal{P}$ is a union of pieces of edge bisectors that is "similar" to the straight skeleton of $\mathcal{P}$. Suppose that partial bisectors $b_1, \ldots, b_n$ meet and end at a vertex v. Let e_i and f_i denote the edges that b_i bisects, ordered to indicate their positions relative to b_i. Then a bisector graph must satisfy that $n \geq 3$, $f_i = e_{i+1}$ for each $1 \leq i < n$, and $f_n = e_1$.

4   Crease Pattern

In addition to the straight skeleton, the crease pattern contains *perpendicular folds*, described in this section. Let us assume that $\mathcal{P}$ is *non-degenerate* in that every internal vertex of the straight skeleton has degree three. Then there are three regions and three edges of the polygon associated with each $v \in I(\mathrm{SS})$.

Let us first consider the perpendicular folds for convex $\mathcal{P}$. For each $v \in I(\mathrm{SS})$, we form a crease emanating from v towards and perpendicular to (the line extension of) each of the three polygon edges corresponding to v.
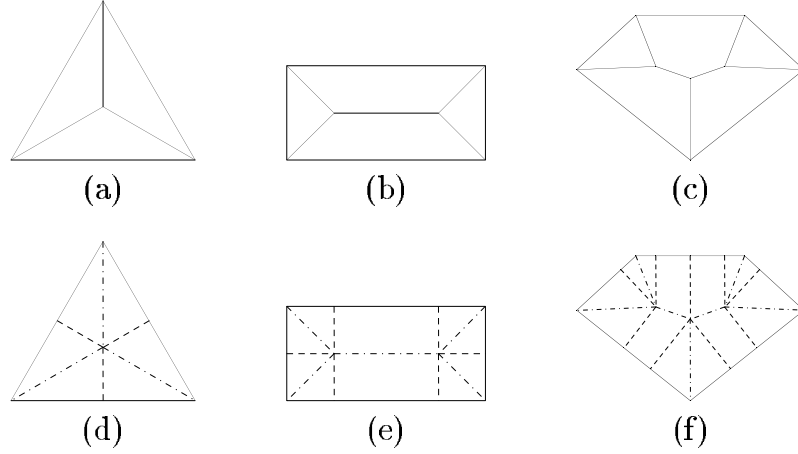
6

Figure 4: *(a–c) Straight skeleton of polygons and (d–f) crease patterns used to generate the extreme bases in Figure 1. Dashed [dot-dashed] segments denote valley [mountain] folds.*

Lemma 2 *If $\mathcal{P}$ is convex, perpendiculars intersect with the polygon boundary before intersecting with any other edges of the crease pattern.*

Examples of the straight skeleton and crease pattern for convex $\mathcal{P}$ are given in Figure 4.

For non-convex $\mathcal{P}$, we use the same construction for most $v \in I(\mathrm{SS})$. For v adjacent to a reflex vertex r of $\mathcal{P}$, however, we only draw one crease, to the edge that does not have r as an endpoint. Finally, there are two more creases that emanate from each reflex vertex r, perpendicular to the two edges that have r as an endpoint.

For non-convex $\mathcal{P}$, a crease may not reach the edge that it is aimed for (and perpendicular to). Instead, a crease c may hit another edge e of the straight skeleton (Figure 5). In this case, we stop c at the intersection point x, and start a new crease emanating from x in the direction obtained by reflecting c about e. The straight skeleton causes these bouncing creases (called *perpendiculars*) to have the following property:

Lemma 3 *A perpendicular will eventually reach an edge of $\mathcal{P}$, and it will be perpendicular to it. For convex $\mathcal{P}$, perpendiculars do not bounce, that is, they reach the edge they originally aim for.*

An example of the crease pattern and resulting extreme base for a non-convex quadrilateral $\mathcal{P}$ is given in Figure 5.

Note that perpendiculars cannot bounce off each other, since

Lemma 4 *A perpendicular crease meets a polygon edge perpendicular to it. Hence, the perpendicular creases are parallel in any region of* SS.

Two perpendiculars may hit each other dead on, but we consider this case a degeneracy and ignore it for the purposes of this paper.
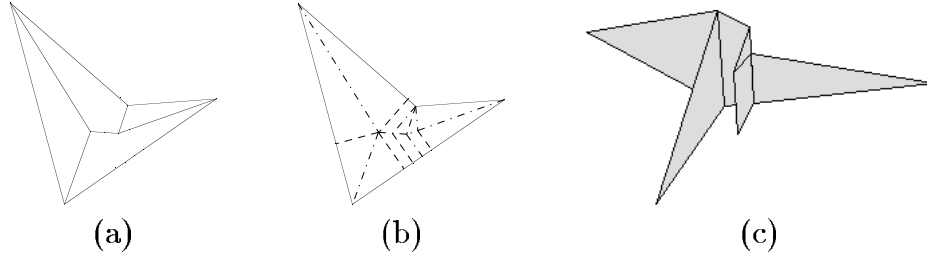
7

Figure 5: *(a) Straight skeleton, (b) crease pattern, and (c) completely folded extreme base for a non-convex quadrilateral.*

We shall now briefly note which creases are valleys and which are mountains, that is, whether a crease folds lower or higher, in the z direction, than its two incident faces. An edge $\{r, s\} \in E(\text{SS})$ incident to a reflex vertex r of $\mathcal{P}$ is assigned to be a valley, and all other $e \in E(\text{SS})$ are mountains. Perpendiculars switch their "direction" each time they bounce. Perpendiculars from reflex vertices r of $\mathcal{P}$ or vertices $s \in V(\text{SS})$ adjacent to reflex vertices are initially mountains, and all other perpendiculars are initially valleys.

This completes what we call the *creasing algorithm*, that is, the algorithm that computes the crease pattern of an extreme base.

4.1 Notation for Convex Polygons

In the next section, we will see how to compute the entire extreme base according to the definition in Section 2, that is, determine how the paper actually folds, if $\mathcal{P}$ is convex. To aid in this construction, we define some notation for the crease pattern for convex $\mathcal{P}$, where perpendiculars are single segments (that is, they do not bounce). In this case, we usually associate perpendiculars with their "ends," that is, the points on the polygon boundary that they reach.

We will use perps(v) to denote the set of perpendiculars that are incident to $v \in V(\text{SS})$. Note that $|\text{perps}(v)| = 3$ if $v \in I(\text{SS})$ and perps(v) = $\emptyset$ otherwise. We denote the edge of $\mathcal{P}$ that $v_1 \in \text{perps}(v)$ is on by edge(v_1).

One useful property is that distinct $v_1, v_2 \in \text{perps}(v)$ determine a neighbor $w \in V(\text{SS})$, denoted by neigh(v_1, v_2). If $w \in I(\text{SS})$, then there are $w_1, w_2 \in \text{perps}(w)$ (denoted by perp(w, v_1) and perp(w, v_2)) that are adjacent to v_1 and v_2, respectively. (Here "adjacent" means that there are no other perpendiculars between v_1 and w_1, or v_2 and w_2.)

Another property that follows by induction is that $|v - v_1|$ is the same for all $v_1 \in \text{perps}(v)$. We denote this common length by plength(v). Note that plength(root(SS)) = max $\{\text{plength}(v) \mid v \in I(\text{SS})\}$.

8

5 Folding Process

Although several researchers have suggested the definitions in Section 2 for foldings [3, 9, 14], no one has yet published such a construction for an infinite class of folds. In this section, we describe the folding process for extreme bases of convex polygons.

5.1 Circles in 3-Space

Much of our movement is defined by circles, so let us first develop some notation for points on circles.

If p and q are two distinct points in 2-space, let $\angle(p,q)$ denote the angle of the oriented segment from p to q with respect to the x axis. This can be defined by $\angle(p,q) = \angle p + (1,0), p, q$ (specified in counter-clockwise order). For example, if $q - p = (0,y)$ where $y < 0$, then $\angle(p,q) = 3\pi/2 \equiv -\pi/2$.

If p is a point in 3-space, let $c[p,\theta,r]$ denote the circle in 3-space perpendicular to the xy plane with center p, radius r, and angle θ with respect to the xz plane. Hence, a point on $c[p,\theta,r]$ can be defined by an angle φ as follows:

$$c[p,\theta,r](\varphi) = p + r(\cos\varphi\cos\theta, \cos\varphi\sin\theta, \sin\varphi).$$

For example, $c[(p,z),\angle(p,q),|p-q|](0) = (q,z)$ and $c[(p,0),\theta,r](-\pi/2) = (p,-r)$.

5.2 Convex Polygons

In this paper, we will only discuss the folding f for a convex paper $\mathcal{P}$, where perpendiculars do not bounce (the construction for non-convex $\mathcal{P}$ is under development). Furthermore, we only consider non-degenerate $\mathcal{P}$ (Section 4).

Since f must be an isometry on each face of the crease pattern, we only need to define it at the vertices of the crease pattern (that is, at each straight-skeleton vertex and perpendicular end). The complete definition of f simply comes from linear interpolation along each edge and in each face. We will define f on the vertices recursively, starting with root(SS) and ending with $v \in L(SS)$. However, we delay the definition of $f(\text{root}(SS),t)$ until the end; for now, assume that it is given.

Suppose that we know the movement of a $v \in I(SS)$ (e.g., $v = \text{root}(SS)$), and let $v_1 \in \text{perps}(v)$. We force v_1 to move along a circle centered at v with radius plength(v), uniformly from angle 0 down to angle $-\pi/2$, keeping in mind that v may be moving. Hence, we define

$$f(v_1,t) = c[f(v,t), \angle(v,v_1), \text{plength}(v)](-t\pi/2).$$

Suppose that $v_1, v_2 \in \text{perps}(v)$, where $v \in I(SS)$ and $f(v,t)$ is already defined, and suppose that parent$(w) = v$, where $w = \text{neigh}(v_1,v_2)$. Then we define $f(w,t) = g[v_1,v_2,w](t)$. Let us now consider the definition of g. We use this indirect definition since we also want to use the same kind of movement (as captured by g) for $w \notin \mathcal{P}$.
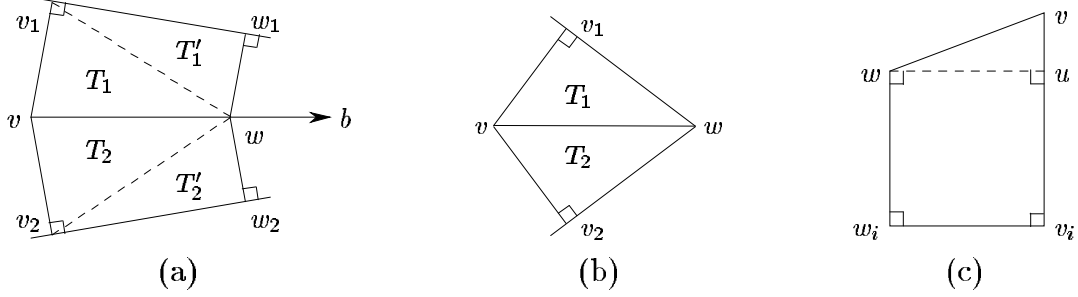
9

Figure 6: *(a–b) Illustration of isometric preservation. w can be any point $\in b - \{v\}$. Here we show two cases, (a) $w \in I(\text{SS})$ and (b) $w \in L(\text{SS})$. (c) Illustration of the property that $f^z(v,t) - f^z(w,t) = |v - u| = |v - v_i| - |w - w_i| = \text{plength}(v) - \text{plength}(w)$.*

Let $v_1, v_2 \in \text{perps}(v)$ be distinct for some $v \in I(\text{SS})$, where $\text{parent}(\text{neigh}(v_1, v_2)) = v$, and suppose that $f(v,t)$ is defined (and hence $f(v_1,t)$ and $f(v_2,t)$ are defined). Let b denote the ray bisecting $\text{edge}(v_1)$ and $\text{edge}(v_2)$, that is, the angular bisector of v_1, v, v_2, pointing towards $\text{neigh}(v_1, v_2)$ (Figure 6(a)). Clearly, $v, \text{neigh}(v_1, v_2) \in b$. We will give a formula for the motion of any point $w \in b - \{v\}$. Note that $-\pi/2 \leq \angle w, v, v_1 = \angle w, v, v_2 \leq \pi/2$, because of the way b is oriented (to point towards a child, which has shorter perpendiculars). Such a point w moves on a circle centered at v, given by

$$g[v_1, v_2, w](t) = c[f(v,t), \angle(v,w), |v - w|](h(t)),$$

where $h(t)$ is yet to be determined; it specifies the "rate of movement" along the circle. Note that $h(t)$ depends on v_1, v_2, w.

We enforce that $h(0) = 0$, that is, $g[v_1, v_2, w](0) = (w, 0)$. We wish to define the rest of h so that $T_1 = \triangle g[v_1, v_2, w](t), f(v,t), f(v_1,t)$ and $T_2 = \triangle g[v_1, v_2, w](t), f(v,t), f(v_2,t)$ are isometrically preserved as t varies (Figure 6(a–b)). By the side-side-side theorem, this is equivalent to ensuring that the distances $|f(v,t) - f(v_1,t)|$, $|f(v,t) - f(v_2,t)|$, $|f(v,t) - g[v_1, v_2, w](t)|$, $|f(v_1,t) - g[v_1, v_2, w](t)|$, and $|f(v_2,t) - g[v_1, v_2, w](t)|$ are constant as t varies. It should be clear that $|f(v,t) - f(v_1,t)|$, $|f(v,t) - f(v_2,t)|$, and $|f(v,t) - g[v_1, v_2, w](t)|$ are each constant since $f(v_1,t)$, $f(v_2,t)$, and $g[v_1, v_2, w](t)$ are defined to be on the appropriate circles centered at $f(v,t)$. Also, $|f(v_1,t) - g[v_1, v_2, w](t)| = |f(v_2,t) - g[v_1, v_2, w](t)|$ since $w \in b$ and $|f(v,t) - f(v_1,t)| = |f(v,t) - f(v_2,t)|$. Hence, we only need to ensure that $|f(v_1,t) - g[v_1, v_2, w](t)|$ is constant in defining $h(t)$.

Lemma 5 *Let $c_1 = c[p, \theta_1, r_1]$ and $c_2 = c[p, \theta_2, r_2]$. Define $\alpha = \theta_1 - \theta_2$ and $d = |c_1(0) - c_2(0)|$. Assume that $\alpha \in [-\pi/2, \pi/2]$ and $\varphi_1, \varphi_2 \in [-\pi/2, 0]$. Then $|c_1(\varphi_1) - c_2(\varphi_2)| = d$ if and only if*

$$\cos \varphi_2 = \frac{|\sin \alpha| + \cos \varphi_1}{|\sin \alpha| \cos \varphi_1 + 1}, \quad \text{and}$$

$$\sin \varphi_2 = -\sqrt{1 - \cos^2 \varphi_2}.$$

10

The proof of this lemma is given in Appendix A. In our case, φ_1 and φ_2 denote $-t\pi/2$ and $h(t)$, respectively. These equations completely determine $h(t)$ in terms of φ_1 (that is, t), and hence define g.

Lemma 6 *Let $i \in \{1,2\}$, and let $w_i = \mathrm{perp}(w, v_i)$. If $w \in L(\mathrm{SS})$, f is an isometry on $\triangle v, v_i, w$. Otherwise, f is an isometry on the trapezoid with vertices v, w, w_i, v_i.*

Proof: The properties of g show that f is an isometry on $T = \triangle v, w, p_i^v$, regardless of whether $w \in L(\mathrm{SS})$. Suppose that $w \in I(\mathrm{SS})$ (Figure 6(a)). Since perpendiculars to a common edge are parallel, $\angle(v, v_i) = \angle(w, w_i)$. Now $f(v_i, t)$ and $f(w_i, t)$ are defined to be on circles having centers at $f(v, t)$ and $f(w, t)$ and angles $\angle(v, v_i)$ and $\angle(w, w_i)$, respectively. Hence, the vectors $f(v_i, t) - f(v, t)$ and $f(w_i, t) - f(w, t)$ have the same direction, proving that $f(v, t)$, $f(w, t)$, $f(w_i, t)$, and $f(v_i, t)$ are coplanar. In addition, $\angle f(w_i, t), f(w, t), f(v, t) = \pi - \angle f(w, t), f(v, t), f(v_i, t)$ (because the two perpendicular vectors have the same direction). Since T is preserved, $\angle f(w, t), f(v, t), f(v_i, t)$, hence $\angle f(w_i, t), f(w, t), f(v, t)$, and hence $\angle f(w_i, t), f(w, t), f(v_i, t)$ is constant. We know that $|f(w_i, t) - f(w, t)|$ is constant (by the circle construction). By the side-angle-side theorem, f is an isometry on $T' = \triangle w, w_i, v_i$. Since f maps T and T' to a common plane, f is an isometry on the desired trapezoid. ■

Now that we know how to recurse, we only need to define $f(r, t)$, where $r = \mathrm{root}(\mathrm{SS})$, which can be done arbitrarily (provided it is continuous in t). The obvious definition is $f(r, t) = (r, 0)$ for any $0 \le t \le 1$, but then f would not be uniaxial since most z coordinates are less than zero. We choose the following definition, which causes the perpendicular ends of r to be on the xy plane:

$$f(r, t) = (r, -\mathrm{plength}(r)\sin(-t\pi/2)) = (r, \mathrm{plength}(r)\sin(t\pi/2)).$$

All that remains is to prove the correctness of f. We first prove the *angle containment* property of the crease pattern.

Lemma 7 *Let $a, b, \ldots, u, v$ be a path in SS of length at least 2. Suppose that $b = \mathrm{neigh}(a_1, a_2)$, where $\mathrm{perps}(a) = \{a_1, a_2, a_3\}$. Let $R(a, b)$ denote the range of angles between $\angle(a, a_1)$ and $\angle(a, a_2)$ that does not include $\angle(a, a_3)$ (we need to specify this since we are dealing with a cyclic order). Then $\angle(u, v) \in R(a, b)$ and $\angle(v, v_1) \in R(a, b)$ for any $v_1 \in \mathrm{perps}(v)$.*

Proof: We will prove this by induction on the length of the path (see Figure 7). It is clear that $\angle(a, b) \in R(a, b)$ and $\angle(b, b_1) \in R(a, b)$ for any $b_1 \in \mathrm{perps}(b)$ (base case). Assume that the path is of the form $a, b, c, \ldots, u, v$ and has length at least 3. The induction hypothesis says that $\angle(u, v) \in R(b, c)$ and $\angle(v, v_1) \in R(b, c)$ for any $v_1 \in \mathrm{perps}(v)$. Since $\mathcal{P}$ is convex, $R(b, c) \subseteq R(a, b)$, and the result follows. ■

Lemma 8 f^{xy} *(and hence f itself) is one-to-one for any fixed $t < 1$.*

Figure 7: *Illustration of the induction in the proof of Lemma 7. Note that $\angle(a,b) \in R(a,b)$, $\angle(b,b_1) \in R(a,b)$, and $R(b,c) \subseteq R(a,b)$.*

Proof: Since f is defined as the linear interpolation of the crease-pattern vertices, it suffices to show that, for any fixed $t < 1$, the xy-projections of any two crease-pattern edges do not intersect.

Note that the angles of the circles are constant, so the angles in the xy projection of straight-skeleton edges are preserved over time. By Lemma 7, $\angle(f^{xy}(u,t), f^{xy}(v,t)) = \angle(u,v) \in R(a,b)$ and $\angle(f^{xy}(v,t), f^{xy}(v_1,t)) = \angle(v,v_1) \in R(a,b)$ for any path $a,b,\ldots,u,v$ in SS and $v_1 \in \text{perps}(v)$.

Let $S(a,b)$ denote the region of the plane defined by an infinite triangle (or *wedge*) that has $f^{xy}(a,t)$ as a vertex and $f^{xy}(a,t), f^{xy}(a_1,t)$ and $f^{xy}(a,t), f^{xy}(a_2,t)$ as parts of edges, where $a_1, a_2 \in \text{perps}(a)$ are such that $\text{neigh}(a_1,a_2) = b$. Note that if $u \in S(a,b)$ and $\angle(u,v) \in R(a,b)$ then $v \in S(a,b)$. Hence, $f^{xy}(u,t), f^{xy}(v,t)$ and $f^{xy}(v,t), f^{xy}(v_1,t) \in S(a,b)$ for any path $a,b,\ldots,u,v$ in SS and $v_1 \in \text{perps}(v)$.

Applying this property to all $a \in I(\text{SS})$ provides a *spatial separation* of the xy-projections of the straight-skeleton perpendicular folds. It is easy to show the same result for edges of $\mathcal{P}$, thereby proving the lemma. ∎

The following is a constructive version of Theorem 1 (for convex polygons $\mathcal{P}$).

Theorem 3 f *is a folding of an extreme base.*

Proof: We must prove that f is a folding, and that the resulting base b is uniaxial and extreme.

Lemma 6 shows that f is an isometry on the faces of the crease pattern. Lemma 8 shows that f satisfies the non-crossing condition. It should be obvious that $f(p,0) = (p,0)$ for all $p \in \mathcal{P}$, since $c[(p,0), \angle(p,q), |p-q|](0) = q$ for all points p,q in 2-space. Hence, f folds a base b, defined by $b(p) = f(p,1)$.

Note that $b(v), b(v_1)$ points in the negative-z direction for each $v \in I(\text{SS})$ and $v_1 \in \text{perps}(v)$ (corresponding to angle $-\pi/2$ on the circle containing v_1). Hence, the faces of f are perpendicular to the xy plane. The xy-projection and the intersection with the xy plane are both equal to the tree with edges $\{b(v_1), b(w_1)\}$, where $v = \text{parent}(w)$ and $w_1 = \text{perp}(w,v_1)$, for all $w \in V(\text{SS})$ and one choice of $v_1 \in \text{perps}(v)$. Therefore, b is uniaxial.

Let $v \in I(\mathrm{SS})$ and $w = \mathrm{neigh}(v_1, v_2)$, where $v_1, v_2 \in \mathrm{perps}(v)$ are distinct and $\mathrm{parent}(w) = v$. Let $i \in \{1, 2\}$, and let $w_i = \mathrm{perp}(w, v_i)$ (Figure 6(c)). If we shoot a ray from w parallel to w_i, v_i (that is, $\mathrm{edge}(v_i) = \mathrm{edge}(w_i)$) and intersect it with v, v_i, we get a vertex u such that $f(w, t), f(u, t)$ is perpendicular to $f(v, t), f(v_i, t)$ (this is clearly true for $t = 0$, and is preserved by Lemma 6). Hence, $|f(v, t) - f(u, t)| = \mathrm{plength}(v) - \mathrm{plength}(w)$ (again, this is clear for $t = 0$ because the two perpendiculars are parallel, and is preserved by Lemma 6). The oriented segments $b(v), b(v_i)$ and $b(w), b(w_i)$ both point in the negative-z direction (argued above). Hence, $b(w), b(u)$ is on a plane parallel to the xy plane, so they have the same z coordinate, and hence $b^z(w) - b^z(v) = \mathrm{plength}(v) - \mathrm{plength}(w)$.

Since $f(v_i, t)$ is $\mathrm{plength}(v)$ lower than $f(v, t)$ in z coordinate (corresponding to angle $-\pi/2$ on the circle containing v), we have that

$$
\begin{aligned}
b^z(v_i) &= b^z(r) - \mathrm{plength}(v) - \sum_{j=1}^{k} \Big(\mathrm{plength}(\mathrm{parent}^j(v)) - \mathrm{plength}(\mathrm{parent}^{j-1}(v)) \Big) \\
&= b^z(r) - \mathrm{plength}(r) \\
&= \mathrm{plength}(r) \left(\sin(\pi/2) - 1 \right) \\
&= 0,
\end{aligned}
$$

where $r = \mathrm{root}(\mathrm{SS})$ and $\mathrm{parent}^k(v) = r$. If we define $\mathrm{plength}(v) = 0$ for $v \in L(\mathrm{SS})$, this also shows that $b^z(v) = 0$. Therefore, b is extreme. ∎

5.3 Flattening Extreme Bases

Finally, to solve the folding-and-cutting problem for convex polygons from these results, we need to be able to "flatten" an extreme base.

Lemma 9 *The base b of f, viewed as the 3-dimensional "paper," can be folded flat. In other words, there exists a function g from $b(\mathcal{P}) \times [0, 1]$ to 3-space that is a flat folding.*

Since each face of $b(\mathcal{P})$ is perpendicular to the xy plane, this is simply a two-dimensional problem of folding a tree (namely the shadow tree) into a line segment. If we disallow extra folds, this is a kind of *linkage* problem [19], constrained so that the links (rigid rods) cannot cross. A recent conjecture, simultaneously made by several people including Sue Whitesides and Joe Mitchell, is that any closed chain of links can be folded in the plane (at no time crossing links) to be convex. We believe that this conjecture is equivalent to that of folding a tree of links into a line segment. In particular, the closed-chain conjecture clearly implies the tree conjecture: simply "thicken" (i.e., split into two segments) each edge of the tree to turn it into a closed chain. For the case of the shadow tree of our extreme bases, however, we can prove "flattenability" without using any extra folds.

Proof: As we noted before, the shadow tree has the same structure and angles as $\mathrm{SS}(\mathcal{P})$, just the lengths of the edges may differ. Find two leaves l_1 and l_2 incident to a common

vertex v (if such leaves do not exist, the shadow tree is already a segment). Let u be the other vertex incident to v. By the spatial separation property (see the proof of Lemma 8), $R(u, v)$ is empty except for l_1 and l_2. In particular, the pie wedge centered at v with radii endpoints l_1 and l_2 contains no links. Hence, there is room to fold the edges (v, l_1) and (v, l_2) together so that they simply extend the edge (u, v). We have thus reduced the problem by effectively removing the two edges l_1 and l_2, except that the lengths of the edges may differ. All relevant properties are therefore preserved, and the desired result follows by induction. ∎

6 Conclusion

In this paper, we have presented an algorithm to construct the crease pattern of a uniaxial base with an arbitrary polygonal paper boundary mapping to a common plane. This significantly generalizes previous results. We feel that the bases form useful molecules, and hence have applications to origami design. So far, we have successfully designed a few origami models using extreme bases.

We have presented a full description of the folding process for an extreme base of a convex polygon. Such descriptions have not been previously made other than for simple folds like those involved in a flapping bird [20]. In our case, they prove the interesting result that our foldings can be performed with rigid faces of paper. In addition, we are able to animate the folding of extreme bases; snapshots are given in Figure 1. We also plan to extend to other origamis; the goal is to develop functions that represent all types of folds. This will require extending our definition of foldings to allow curving.

Extreme bases by themselves, the topic of this paper, allow us to solve the folding-and-cutting problem directly only for convex polygons, since otherwise we must deal with the outside of the polygon in addition. Our current work is on solving the general problem of an arbitrary arrangement of line segments. In particular, we have nearly completed the solution for non-convex polygons.

We conclude with a conjecture relating to extreme bases, the latter part of which was suggested by Jeff Erickson.

Conjecture 1 *Any extreme base for a simple polygon $\mathcal{P}$ includes a bisector graph as part of its crease pattern. Conversely, there exists an extreme base using any given bisector graph of $\mathcal{P}$.*

Acknowledgment

us with a number of origami-mathematics papers. This work was supported by the Natural Science and Engineering Research Council (NSERC).

References

[1] Oswin Aichholzer and Franz Aurenhammer. Straight skeletons for general polygonal figures in the plane. In *Proceedings of the 2nd Annual International Conference on Computing and Combinatorics (COCOON'96)*, volume 1090 of *Lecture Notes in Computer Science*, pages 117–126. Springer, 1996.

[2] Oswin Aichholzer, Franz Aurenhammer, David Alberts, and Bernd Gärtner. A novel type of skeleton for polygons. *Journal of Universal Computer Science*, 1(12):752–761, 1995.

[3] Marshall Bern and Barry Hayes. The complexity of flat origami. In *Proceedings of the 7th Annual ACM-SIAM Symposium on Discrete Algorithms*, pages 175–183, Atlanta, January 1996.

[4] H. Blum. A transformation for extracting new descriptors of shape. In W. Whaten-Dunn, editor, *Proceedings of the Symposium on Models for Perception of Speech and Visual Form*, pages 362–380. MIT Press, 1967.

[5] David Eppstein and Jeff Erickson. Raising roofs, crashing cycles, and playing pool: Applications of a data structure for finding pairwise interactions. Submitted to 14th ACM Symposium on Computational Geometry, Minneapolis/St. Paul, June, 1998.

[6] Martin Gardner. Paper cutting. In *New Mathematical Diversions (Revised Edition)*, Spectrum Series, chapter 5, pages 58–69. The Mathematical Association of America, Washington, D.C., 1995.

[7] Robert Geretschläger. Euclidean constructions and the geometry of origami. *Mathematics Magazine*, 68(5):357–371, 1995.

[8] Harry Houdini. *Paper Magic*, pages 176–177. E. P. Dutton & Company, 1922.

[9] Thomas Hull. On the mathematics of flat origamis. *Congressum Numerantium*, 100:215–224, 1994.

[10] Thomas Hull. Personal communication, January 1997.

[11] Humiaki Huzita and Benedetto Scimemi. The algebra of paper folding (origami). In H. Huzita, editor, *Proceedings of the 1st International Meeting of Origami Science and Technology*, pages 215–222, Ferrara, Italy, December 1989.

[12] Jacques Justin. Towards a mathematical theory of origami. In Koryo Miura, editor, *Proceedings of the 2nd International Meeting of Origami Science and Scientific Origami*, pages 15–29, Otsu, Japan, November–December 1994.

[13] Toshikazu Kawasaki. On the relation between mountain-creases and valley-creases of a flat origami. In H. Huzita, editor, *Proceedings of the 1st International Meeting of Origami Science and Technology*, pages 229–337, Ferrara, Italy, December 1989. An unabridged Japanese version appeared in *Sasebo College of Technology Report*, 27:153–157, 1990.

[14] Robert J. Lang. A computational algorithm for origami design. In *Proceedings of the 12th Annual Symposium on Computational Geometry*, pages 98–105, Philadelphia, PA, May 1996.

[15] Gerald M. Loe. *Paper Capers*. Magic, Inc., Chicago, 1955.

[16] E. A. Lord and C. B. Wilson. *The Mathematical Description of Shape and Form*. Ellis Horwood Limited, West Sussex, England, 1984.

[17] Jun Maekawa. Evolution of origami organisms. *Symmetry: Culture and Science*, 5(2):167–177, 1994.

[18] Joseph O'Rourke. *Computational Geometry in C*, pages 193–195. Cambridge University Press, 1994.

[19] Sue Whitesides. Algorithmic issues in the geometry of planar linkage movement. *Australian Computer Journal*, 24(2):42–50, May 1992.

[20] Liudmila I. Zamiatina. Computer simulations of origami. *Mathematica in Education*, 3(3):23–31, Summer 1994.

A   Distance-Preserving Movement on Two Circles

This appendix provides a derivation and proof of Lemma 5.

Suppose that we have two circles C_1 and C_2 in 3-space that are both perpendicular to the xy plane and have a common center point. Let r_1 and r_2 denote their radii, respectively. Without loss of generality, translate so that the center point is the origin, and rotate to make C_1 on the xz plane. Hence, an arbitrary point on C_1 has the coordinates

$$(r_1 \cos \varphi_1, 0, r_1 \sin \varphi_1)$$

where φ_1 is a parameter, $0 \leq \varphi_1 < 2\pi$.

C_2 is defined parametrically by

$$(r_2 \cos \varphi_2 \cos \alpha, r_2 \cos \varphi_2 \sin \alpha, r_2 \sin \varphi_2)$$

where φ_2 is a parameter with the same bounds as φ_1. Note that α is the angle between the planes of C_1 and C_2.

For given values of φ_1 and φ_2, we can compute the square of the Euclidean distance between the corresponding points on the circles:

$$
\begin{aligned}
& (r_1 \cos \varphi_1 - r_2 \cos \varphi_2 \cos \alpha)^2 + (r_2 \cos \varphi_2 \sin \alpha)^2 + (r_1 \sin \varphi_1 - r_2 \sin \varphi_2)^2 \\
= \ & (r_1^2 \cos^2 \varphi_1 - 2r_1 r_2 \cos \varphi_1 \cos \varphi_2 \cos \alpha + r_2^2 \cos^2 \varphi_2 \cos^2 \alpha) + \\
& \quad (r_2^2 \cos^2 \varphi_2 \sin^2 \alpha) + (r_1^2 \sin^2 \varphi_1 - 2r_1 r_2 \sin \varphi_1 \sin \varphi_2 + r_2^2 \sin^2 \varphi_2) \\
= \ & r_1^2 + r_2^2 - 2r_1 r_2 (\cos \varphi_1 \cos \varphi_2 \cos \alpha + \sin \varphi_1 \sin \varphi_2).
\end{aligned} \tag{1}
$$

We want to restrict φ_2 with respect to φ_1 such that this distance is constant. We are only interested in the case when $\varphi_1 \in [-\pi/2, 0]$. Substituting $\varphi_1 = \varphi_2 = 0$ into (1) gives the desired distance

$$
d = r_1^2 + r_2^2 - 2r_1 r_2 \cos \alpha.
$$

Since (1) must equal d,

$$
\begin{aligned}
\cos \alpha & = \cos \varphi_1 \cos \varphi_2 \cos \alpha + \sin \varphi_1 \sin \varphi_2 \\
\Rightarrow \ \cos \alpha (1 - \cos \varphi_1 \cos \varphi_2) & = \sin \varphi_1 \sin \varphi_2 \\
\Rightarrow \ \cos^2 \alpha (1 - \cos \varphi_1 \cos \varphi_2)^2 & = (1 - \cos^2 \varphi_1)(1 - \cos^2 \varphi_2)
\end{aligned}
$$

Let a, s, and t denote $\cos \alpha$, $\cos \varphi_1$, and $\cos \varphi_2$, respectively. Rewriting,

$$
\begin{aligned}
a^2 (1 - st)^2 & = (1 - s^2)(1 - t^2) \\
\Rightarrow \ (a^2 s^2 + 1 - s^2) t^2 - (2a^2 s) t + (a^2 - 1 + s^2) & = 0.
\end{aligned}
$$

We can then solve for t using the quadratic formula.

$$
\begin{aligned}
t & = \frac{a^2 s \pm \sqrt{a^4 s^2 - (a^2 - 1 + s^2)(a^2 s^2 + 1 - s^2)}}{a^2 s^2 + 1 - s^2} \\
& = \frac{a^2 s \pm \sqrt{s^4 (1 - a^2) - 2s^2 (1 - a^2) + (1 - a^2)}}{a^2 s^2 + 1 - s^2} \\
& = \frac{a^2 s \pm (1 - s^2)\sqrt{1 - a^2}}{a^2 s^2 + 1 - s^2};
\end{aligned}
$$

that is,

$$
\begin{aligned}
\cos \varphi_2 & = \frac{\cos^2 \alpha \cos \varphi_1 \pm \sin^2 \varphi_1 \sin \alpha}{\cos^2 \alpha \cos^2 \varphi_1 + \sin^2 \varphi_1} \\
& = \frac{(1 - \sin^2 \alpha) \cos \varphi_1 \pm (1 - \cos^2 \varphi_1) \sin \alpha}{(1 - \sin^2 \alpha) \cos^2 \varphi_1 + (1 - \cos^2 \varphi_1)} \\
& = \frac{\cos \varphi_1 \pm \sin \alpha - \sin^2 \alpha \cos \varphi_1 \mp \sin \alpha \cos^2 \varphi_1}{1 - \sin^2 \alpha \cos^2 \varphi_1}
\end{aligned}
$$

17

$$\begin{aligned}
&= \frac{(\sin\alpha \pm \cos\varphi_1)(-\sin\alpha\cos\varphi_1 \pm 1)}{(1+\sin\alpha\cos\varphi_1)(1-\sin\alpha\cos\varphi_1)} \\
&= \frac{\sin\alpha \pm \cos\varphi_1}{\sin\alpha\cos\varphi_1 \pm 1}.
\end{aligned} \tag{2}$$

Since we know that $-\pi/2 \le \varphi_2 \le 0$, this completely determines φ_2 in terms of φ_1 and α, aside from the choice of sign ($+$ or $-$).

To decide between the sign, let us examine the case where $\varphi_1 = -\pi/2$, which implies that $\cos\varphi_2 = \pm\sin\alpha$ by (2). Now

$$\varphi_2 = -|\cos^{-1}(\pm\sin\alpha)| = -|\pi/2 \mp \alpha|$$

since $\varphi_2 \in [-\pi/2, 0]$. We only need to deal with the case where $\alpha \in [-\pi/2, \pi/2]$, that is, the circles' planes are no more than $\pi/2$ apart. Since $\varphi_2 \in [-\pi/2, 0]$, we must choose $\mp$ to be $-$ if $\alpha \in [0, \pi/2]$, and choose $\mp$ to be $+$ if $\alpha \in [-\pi/2, 0]$. That is, we choose $\pm$ to be the sign of $\sin\alpha$. Hence,

$$\cos\varphi_2 = \frac{|\sin\alpha| + \cos\varphi_1}{|\sin\alpha|\cos\varphi_1 + 1}. \tag{3}$$

We must ensure that (3) is solvable in all cases that we are interested in. The denominator is never 0 since $-\pi/2 \le \varphi_1 \le 0$. Hence, we must ensure that its range is at most $[-1, 1]$ (since $\cos\varphi_2 \in [-1, 1]$). To do so, we can solve

$$\frac{\partial\cos\varphi_2}{\partial\varphi_1} = \frac{-\sin\varphi_1(1 - |\sin\alpha|^2)}{(|\sin\alpha|\cos\varphi_1 + 1)^2} = 0.$$

Since the denominator of this is never zero (using the same reasoning as for the denominator of (3)), this is equivalent to solving

$$\sin\varphi_1(1 - |\sin\alpha|^2) = \sin\varphi_1(1 - \sin^2\alpha) = \sin\varphi_1\cos^2\alpha = 0.$$

This is true if $\varphi_1 = 0$ or $\alpha = \pm\pi/2$. Plugging either of these into (3) gives the value 1. We must also check the boundary values, where $\varphi_1 = \pm\pi/2$ or $\alpha = 0$. Plugging these into (3) gives the values $|\sin\alpha|$ and $\cos\varphi_1$, respectively. Therefore, the range is $[-1, 1]$.